JOURNAL OF THERMOPHYSICS AND HEAT TRANSFER
Vol. 13, No. 1, January–March 1999

Transient Thermal Analysis of Parallel Translucent Layers by Using Green's Functions

Robert Siegel*
NASA Lewis Research Center, Cleveland, Ohio 44135

An analysis is developed for computing transient thermal behavior in a composite of two parallel translucent layers with a space between them. The radiative two-flux equation is coupled with the transient energy equation, and both equations are solved by using Green's functions. Illustrative results are provided for transient heating of two parallel translucent layers that exchange radiation. The external boundaries of the two-layer combination are each exposed to a radiative environment, and all boundaries can be convectively heated or cooled. The layer refractive indices are larger than one, and internal reflections are included with boundaries assumed diffuse. The analysis includes internal emission, absorption, isotropic scattering, and heat conduction. Transient results from the present method are verified for a single gray layer by comparison with a finite difference solution that incorporates a numerical solution of the exact radiative transfer equations for the radiative heat source. Illustrative transient temperature distributions show the effects of an insulating gap between layers, when one side of the two-layer composite is subjected to heating by radiation and convection, while the other side is being cooled.

Nomenclature

a_j = absorption coefficient of translucent material, m^{-1}
c = specific heat of translucent material, J/kg K
D = thickness of each parallel translucent layer (half-thickness of single layer), m
G = flux quantity $2(q_r^+ + q_r^-)$, W/m^2
$\tilde{G}$ = $G/\sigma T_i^4$
ge = Green's function for transient energy equation
gs = Green's function for radiative heat source
H = dimensionless parameter, $h/\sigma T_i^3$
h_{j1}, h_{j2} = convective heat transfer coefficients at $x_j = 0$ and D (Fig. 1), W/m^2 K
K_j = extinction coefficient, $a_j + \sigma_{sj}$, m^{-1}
k_j = thermal conductivity of each layer, W/m K
m_j = the quantity $[3\kappa_{Dj}^2(1 - \Omega_j)]^{1/2}$
N_j = conduction–radiation parameter, $k_j/4\sigma T_i^3 D$
n_j = refractive index of translucent material
P_j = the quantity $(2/3\kappa_{Dj})[(1 + \rho_j^i)/(1 - \rho_j^i)]$
q_r = radiative flux in the x direction, W/m^2
$\tilde{q}_r$ = $q_r/\sigma T_i^4$
q_{r1}, q_{r2} = external radiation fluxes σT_{s1}^4 and σT_{s2}^4 incident at $x_1 = 0$ and $x_2 = D$ ($x = 0$ and $x = 2D$ for a single layer), W/m^2
$\tilde{q}_{r1}$, $\tilde{q}_{r2}$ = dimensionless radiation fluxes, $q_{r1}/\sigma T_i^4$ and $q_{r2}/\sigma T_i^4$
q_r^+, q_r^- = radiative fluxes in positive and negative x directions, W/m^2
Ri = quantity, $(1 + \rho^i)/(1 - \rho^i)$
Ro = quantity, $(1 - \rho^o)/(1 - \rho^i)$
T = absolute temperature, K
T_{gj1}, T_{gj2} = gas temperatures for convection at boundaries (Fig. 1), K
T_i = initial uniform temperature (used as a reference temperature), K
T_{s1}, T_{s2} = temperatures of blackbody radiative surroundings at $x = 0$ and D ($x = 0$ and $x = 2D$ for a single layer), K
t = dimensionless temperature, T/T_i
t_{gj} = dimensionless gas temperatures, T_{gj}/T_i
X_j = x_j/D
x_j = coordinate in each layer (Fig. 1), m
Θ = time, s
θ = dummy integration variable for dimensionless time
κ_{Dj} = optical thickness of one parallel layer, $(a_j + \sigma_{sj})D = K_jD$
ξ = dummy integration variable for X
ρ = density of translucent material, kg/m^3
ρ^o, ρ^i = external and internal reflectivities at a translucent boundary
σ = Stefan–Boltzmann constant, W/m^2 K^4
σ_{sj} = scattering coefficient in layer, m^{-1}
τ = dimensionless time, $(4\sigma T_i^3/\rho cD)\Theta$
Ω = scattering albedo, $\sigma_s/(a + \sigma_s)$

Subscripts

g = gas
j = designates first and second parallel layers, $j = 1$ and 2
11, 12 = at boundaries of first layer (Fig. 1)
21, 22 = at boundaries of second layer (Fig. 1)

Introduction

FOR hot materials that are translucent, such as some ceramics, thermal radiation can significantly influence internal temperature distributions. For transients, heating and cooling behavior with radiative transfer has been studied much less than for a steady state. Detailed transient solutions are needed to examine the heat transfer and thermal stress behavior of ceramic components for high-temperature use, thermal protection coatings, porous insulation systems, and tempering of glass windows. For example, the experiments in Refs. 1 and 2 illustrate the importance of internal radiative transfer during transient cooling of glass. A review of the transient heat transfer literature with radiative transfer is in Ref. 3. To obtain transient solutions, numerical procedures such as finite differ-

Received April 30, 1998; revision received July 7, 1998; accepted for publication July 8, 1998.

*Senior Research Scientist, Research and Technology Directorate, 21000 Brookpark Road. E-mail: robert.siegel@lerc.nasa.gov. Fellow AIAA.

ence and finite element methods have been used to solve the transient energy equation coupled with radiative transfer relations that provide an internal heat source. Both exact and approximate equations have been used for the radiative transfer relations.

Transient solutions were obtained in Ref. 4 for a plane layer with a refractive index larger than one, and with external convection and radiation at each boundary. The exact radiative transfer equations were solved numerically, and these results are used to verify the accuracy of the present method using Green's functions for evaluating the internal radiative heat source and for solving the transient energy equation. Some transient results using two Green's functions were obtained for much different conditions in Ref. 5 for a gray layer in the annular space between two long concentric cylinders. The boundaries were diffuse with specified emissivities, and the medium refractive index was one. Initially, the medium was at a uniform temperature, and each boundary was then suddenly changed to a different temperature.

The two-flux method is used as a simplification for obtaining the radiative heat source term in the energy equation. For the general boundary conditions of external convection and radiation for a layer with diffuse surfaces having unspecified temperatures, it has been demonstrated that the two-flux method predicts accurate transient and steady-state temperature distributions and heat fluxes.[6,7] An advantage of the two-flux method is that isotropic scattering is included without any additional complications. The formulation here using the two-flux method is written for gray layers, but can be applied for nongray properties. Using the relations in Refs. 6 and 8, the Green's functions for the two-flux method can be evaluated in spectral bands to obtain the radiative heat source including spectral property variations, such as for zirconia.[8] Illustrative results are given here to show the transient heating of parallel gray layers separated by an internal space, as compared with a single layer having the same total optical thickness and external heating conditions. Radiation is exchanged between the translucent layers across the internal space that can substantially modify the transient heating from that in a single layer.

Analysis

The two plane layers in Fig. 1 are absorbing dielectrics, such as a ceramic like zirconia, that are translucent, isotropically scattering, heat conducting, and have refractive indices larger than one. There are many parameters for transient solutions in two parallel layers. For simplicity, the thickness D, and the properties c and ρ that are incorporated into the dimensionless time, are specified as being equal for both layers, although the formulation is generalized without difficulty to layers with differing values of these properties. All boundaries of the layers

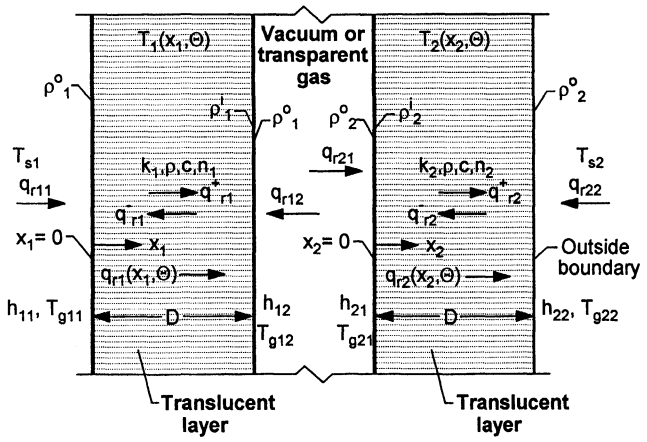

Fig. 1 Geometry and nomenclature for transient radiation and conduction in two parallel translucent layers with a separating space, and boundaries subjected to radiation and convection.

are assumed diffuse. For the results given here and for the nondimensionalization used, both layers are initially at a uniform temperature T_i, but the theory applies for arbitrary initial temperature distributions where T_i is then chosen as a characteristic reference temperature.

To begin a transient, the composite is subjected to surroundings so that each external boundary of the two-layer combination can receive radiant energy and be in contact with a transparent gas that provides convective heating or cooling. There is radiative exchange across the internal space between the layers, and there can also be forced convection by flow in that space. Transient temperature distributions are obtained in the composite until steady state is approached, corresponding to the imposed radiation and convection conditions. Steady-state results were also independently calculated using the steady-state solution method in Ref. 9, with modifications for the boundary conditions here.

Energy Equation and Two-Flux Relations for a Two-Layer Composite

The energy equation in dimensionless form for transient temperatures in each layer is[6]

$$\frac{\partial t_j}{\partial \tau} = N_j \frac{\partial^2 t_j}{\partial X_j^2} - \frac{1}{4}\frac{\partial \tilde{q}_{rj}}{\partial X_j}, \qquad j = 1, 2 \tag{1}$$

where $-(1/4)\partial\tilde{q}_{rj}(X_j, \tau)/\partial X_j$ is the local radiative heat source from absorption, emission, and scattering. Properties are assumed independent of temperature. The $\partial\tilde{q}_{rj}(X_j, \tau)/\partial X_j$ is obtained in terms of $t_j(X_j, \tau)$ and the surrounding radiative conditions, from the two-flux relations that have been found to provide accurate results in previous transient and steady-state studies.[6,7] For each layer of the composite, the two-flux equations using the Milne–Eddington approximation are[6]

$$\frac{\partial \tilde{q}_{rj}(X_j, \tau)}{\partial X_j} = \kappa_{Dj}(1 - \Omega_j)[4n_j^2 t_j^4(X_j, \tau) - \tilde{G}_j(X_j, \tau)], \quad j = 1, 2 \tag{2a}$$

with $\tilde{G}_j(X_j, \tau)$ related to the radiative flux $\tilde{q}_{rj}(X_j, \tau)$ by

$$\frac{\partial \tilde{G}_j(X_j, \tau)}{\partial X_j} = -3\kappa_{Dj}\tilde{q}_{rj}(X_j, \tau) \tag{2b}$$

The $\tilde{q}_{rj}(X_j, \tau)$ and $\tilde{G}_j(X_j, \tau)$ are related to the positive and negative radiative fluxes in Fig. 1 by $\tilde{q}_{rj} = \tilde{q}_{rj}^+ - \tilde{q}_{rj}^-$ and $\tilde{G}_j = 2(\tilde{q}_{rj}^+ + \tilde{q}_{rj}^-)$.

Boundary and Initial Conditions

For a translucent material there is radiant absorption only within the material interior, so that the conduction and convection conditions at the layer boundaries are

$$\left.\frac{\partial t_j}{\partial X_j}\right|_{X_j=0} = -\frac{H_{j1}}{4N_j}[t_{gj1} - t_j(0, \tau)] \tag{3a}$$

$$\left.\frac{\partial t_j}{\partial X_j}\right|_{X_j=1} = -\frac{H_{j2}}{4N_j}[t_j(1, \tau) - t_{gj2}] \tag{3b}$$

The radiative boundary conditions must include the effects of external and internal reflections at the surfaces that have incident external fluxes q_{rj1} and q_{rj2}. By considering incident and reflected fluxes at and across an interface, the following boundary relations between $\tilde{G}$ and $\tilde{q}_r$ were developed[7]:

$$\tilde{G}_j(0, \tau) = 4Ro_j\tilde{q}_{rj1} - 2Ri_j\tilde{q}_{rj}(0, \tau) \tag{4a}$$

$$\tilde{G}_j(1, \tau) = 4Ro_j\tilde{q}_{rj2} + 2Ri_j\tilde{q}_{rj}(1, \tau) \tag{4b}$$

The initial condition for the results given here is a uniform temperature, and so $t_j(X_j, 0) = T_j(x_j, 0)/T_i = 1$, but the method

is valid for an arbitrary $t_j(X_j, 0)$ with T_i then chosen as a characteristic reference temperature.

Green's Function for $\partial\tilde{q}_r(X, \tau)/\partial X$ for a Gray Layer

To develop the Green's function, Eq. (2b) is differentiated in X_j and is used to eliminate $\partial\tilde{q}_{rj}(X_j, \tau)/\partial X_j$ from Eq. (2a); this yields a second-order equation for $\tilde{G}_j(X_j, \tau)$

$$\frac{d^2\tilde{G}_j}{dX_j^2} - m_j^2\tilde{G}_j(X_j, \tau) = -4m_j^2n_j^2t_j^4(X_j, \tau) \tag{5}$$

where $m_j^2 = 3\kappa_{Dj}^2(1 - \Omega_j)$. In Ref. 6, a Green's function was developed that can be used to find solutions for Eq. (5) that satisfy the radiative boundary conditions in Eqs. (4a) and (4b). The final form of the Green's function is as follows, where the τ functional notation is omitted for convenience:

$$gs_j(X_j, \xi) = \begin{cases} \left[\dfrac{\sinh m_j(1 - \xi) + P_jm_j\cosh m_j(1 - \xi)}{2P_jm_j\cosh m_j + (1 + P_j^2m_j^2)\sinh m_j}\right][\sinh m_jX_j + P_jm_j\cosh m_jX_j], & 0 \le X_j < \xi \\ \left[\dfrac{\sinh m_j\xi + P_jm_j\cosh m_j\xi}{2P_jm_j\cosh m_j + (1 + P_j^2m_j^2)\sinh m_j}\right][\sinh m_j(1 - X_j) + P_jm_j\cosh m_j(1 - X_j)], & \xi < X_j \le 1 \end{cases} \tag{6}$$

The $gs_j(X_j, \xi)$ in Eq. (6) is used to account for the nonhomogeneous term in Eq. (5) when computing $\tilde{G}_j(X_j, \tau)$ at each time step during the transient. To obtain the complete solution for $\tilde{G}_j(X_j, \tau)$, the solution is also needed for the homogeneous part of Eq. (5). This was developed in Ref. 6 as

$$\tilde{G}h_j(X_j) = \frac{4Ro_j}{2P_jm_j\cosh m_j + (1 + P_j^2m_j^2)\sinh m_j} \times \{[\sinh m_j(1 - X_j) + P_jm_j\cosh m_j(1 - X_j)]\tilde{q}_{rj1} + (\sinh m_jX_j + P_jm_j\cosh m_jX_j)\tilde{q}_{rj2}\} \tag{7}$$

By adding $\tilde{G}h_j(X_j)$ and the nonhomogeneous solution obtained using $gs_j(X_j, \xi)$, the general solution of Eq. (5) at each time is

$$\tilde{G}_j(X_j, \tau) = \tilde{G}h_j(X_j) + 4m_jn_j^2\int_0^1 gs_j(X_j, \xi)t_j^4(\xi, \tau)\,d\xi, \quad j = 1, 2 \tag{8}$$

The $\tilde{G}_j(X_j, \tau)$ is substituted into Eq. (2a) along with $t_j(X_j, \tau)$ to evaluate $\partial\tilde{q}_{rj}(X_j, \tau)/\partial X_j$, which is used in Eq. (1) to solve for the temperature distribution at the next time step.

The relations provided here for a gray material can be further developed for transient solutions in materials with properties that vary with radiation frequency. Relations for using two spectral bands are in Refs. 6 and 8, and these can be directly extended to more bands.

Radiative Exchange Fluxes in Space Between Layers

The incident radiative fluxes in the internal space between the two layers are shown in Fig. 1; each consists of energy transmitted through the surface of the opposite translucent layer and energy reflected from the opposing layer:

$$\tilde{q}_{r12}(\tau) = (1 - \rho_2^i)\tilde{q}_{r2}^-(0, \tau) + \rho_2^o\tilde{q}_{r21}(\tau) \tag{9a}$$

$$\tilde{q}_{r21}(\tau) = (1 - \rho_1^i)\tilde{q}_{r1}^+(1, \tau) + \rho_1^o\tilde{q}_{r12}(\tau) \tag{9b}$$

The fluxes $\tilde{q}_{r1}^+(1, \tau)$ and $\tilde{q}_{r2}^-(0, \tau)$ inside the translucent layers at the boundaries of the separating space are related to the radiative flux quantities $\tilde{q}_{rj}$ and $\tilde{G}_j$ by the functions[7]

$$\tilde{q}_{r1}^+(1, \tau) = \frac{1}{2}\left[\frac{\tilde{G}_1(1, \tau)}{2} + \tilde{q}_{r1}(1, \tau)\right] \tag{10a}$$

$$\tilde{q}_{r2}^-(0, \tau) = \frac{1}{2}\left[\frac{\tilde{G}_2(0, \tau)}{2} - \tilde{q}_{r2}(0, \tau)\right] \tag{10b}$$

From the boundary conditions, Eqs. (4a) and (4b), additional relations are provided between the incident radiative fluxes and the $\tilde{G}$ values at the boundaries

$$\tilde{q}_{r1}(1, \tau) = \frac{1}{2Ri_1}[\tilde{G}_1(1, \tau) - 4Ro_1\tilde{q}_{r12}] \tag{11a}$$

$$\tilde{q}_{r2}(0, \tau) = -\frac{1}{2Ri_2}[\tilde{G}_2(0, \tau) - 4Ro_2\tilde{q}_{r21}] \tag{11b}$$

Combining Eqs. (9–11), the $\tilde{q}_{r1}^+(1, \tau)$, $\tilde{q}_{r2}^-(0, \tau)$, $\tilde{q}_{r1}(1, \tau)$, and $\tilde{q}_{r2}(0, \tau)$ are eliminated to yield the following relations for incident fluxes $\tilde{q}_{r12}(\tau)$ and $\tilde{q}_{r21}(\tau)$ in the space between the layers:

$$\tilde{q}_{r12}(\tau) = \frac{1}{2\text{ Denom}}\left[\frac{\tilde{G}_2(0, \tau)}{Ri_2} - \frac{\tilde{G}_1(1, \tau)}{Ri_1}\left(\frac{1}{Ri_2} - \frac{2\rho_2^o}{1 + \rho_2^i}\right)\right] \tag{12a}$$

$$\tilde{q}_{r21}(\tau) = \frac{1}{2\text{ Denom}}\left[\frac{\tilde{G}_1(1, \tau)}{Ri_1} - \frac{\tilde{G}_2(0, \tau)}{Ri_2}\left(\frac{1}{Ri_1} - \frac{2\rho_1^o}{1 + \rho_1^i}\right)\right] \tag{12b}$$

where

$$\text{Denom} = 1 - \left(\frac{1}{Ri_1} - \frac{2\rho_1^o}{1 + \rho_1^i}\right)\left(\frac{1}{Ri_2} - \frac{2\rho_2^o}{1 + \rho_2^i}\right)$$

Green's Function for Transient Energy Equation

Green's function, $ge(X, \tau)$, for the transient solution of the energy equation in a layer with convective boundary conditions and an internal heat source is given in Ref. 10, and the relations required for the present results are briefly summarized here. The form given applies for small changes in time, which is convenient to use here for moving ahead each small time increment. Green's function is written in three parts, and so for each translucent layer, $ge(X_j, \tau, \xi, \theta) = ge1(X_j, \tau, \xi, \theta) + ge2(X_j, \tau, \xi, \theta) + ge3(X_j, \tau, \xi, \theta)$, where

$$ge1(X_j, \tau, \xi, \theta) = \frac{1}{\sqrt{4\pi N_j(\tau - \theta)}}\left\{\exp\left[-\frac{(X_j - \xi)^2}{4N_j(\tau - \theta)}\right] + \exp\left[-\frac{(X_j + \xi)^2}{4N_j(\tau - \theta)}\right] + \exp\left[-\frac{(2 - X_j - \xi)^2}{4N_j(\tau - \theta)}\right]\right\} \tag{13a}$$

$$ge2(X_j, \tau, \xi, \theta) = -\frac{H_{j1}}{4N_j}\exp\left[\frac{H_{j1}(X_j + \xi)}{4N_j} + \frac{H_{j1}^2}{16N_j}(\tau - \theta)\right] \times \text{erfc}\left[\frac{X_j + \xi}{\sqrt{4N_j(\tau - \theta)}} + \frac{H_{j1}}{4\sqrt{N_j}}\sqrt{\tau - \theta}\right] \tag{13b}$$

$$ge3(X_j, \tau, \xi, \theta) = -\frac{H_{j2}}{4N_j}\exp\left[\frac{H_{j2}(2 - X_j - \xi)}{4N_j} + \frac{H_{j2}^2}{16N_j}(\tau - \theta)\right] \times \text{erfc}\left[\frac{2 - X_j - \xi}{\sqrt{4N_j(\tau - \theta)}} + \frac{H_{j2}}{4\sqrt{N_j}}\sqrt{\tau - \theta}\right] \tag{13c}$$

Temperatures in each layer are then found by integrating Green's function in the form

$$t_j(X_j, \tau + \Delta\tau) = \int_0^1 ge(X_j, \tau + \Delta\tau, \xi, \tau) t_j(\xi, \tau)\, d\xi - \frac{1}{4}\int_\tau^{\tau+\Delta\tau}\int_0^1 \frac{\partial \tilde{q}_{rj}(\xi, \theta)}{\partial X_j} ge(X_j, \tau + \Delta\tau, \xi, \theta)\, d\xi\, d\theta + \frac{1}{4}\int_\tau^{\tau+\Delta\tau} [H_{j1} t_{gj1} ge(X_j, \tau + \Delta\tau, 0, \theta) + H_{j2} t_{gj2} ge(X_j, \tau + \Delta\tau, 1, \theta)]\, d\theta \quad (14)$$

Numerical Evaluation

Starting with the initial $t_j(X_j, 0) = 1$, and with the initial radiative fluxes in the space between the layers, $\tilde{q}_{r12} = \tilde{q}_{r21} = 1$, the Green's function in Eq. (6) and the homogeneous solution from Eq. (7) are used to obtain $\tilde{G}_j(X_j, 0)$ by evaluating the integral in Eq. (8) for each layer. The $\partial\tilde{q}_{rj}(X_j, 0)/\partial X_j$ is then evaluated from Eq. (2a). The energy equation, Eq. (1), for $t_j(X_j, \tau)$ in each layer is then integrated forward in time using the Green's function relations in Eqs. (13) and (14). This yields $t_j(X_j, \tau + \Delta\tau)$ in each layer. To continue onto the next time step, new values of the fluxes $\tilde{q}_{r12}$ and $\tilde{q}_{r21}$ that are exchanged between the layers are calculated from Eqs. (12).

After advancing $t_j(X_j, \tau)$ each $\Delta\tau$, the radiant flux gradient for use in the energy equation is advanced to $\tau + \Delta\tau$ by using the Green's function solution in Eqs. (6–8) to obtain $\tilde{G}_j(X_j, \tau + \Delta\tau)$, and then evaluating Eq. (2a) using $t_j(X_j, \tau + \Delta\tau)$. The $t(X, \tau)$ is then farther advanced to the next $\Delta\tau$ using Eqs. (13) and (14). Double precision was used for evaluating the integrals involving Green's functions using integration subroutines. Accuracies of integrals were checked by comparing Gaussian and Romberg integrations in the program and checking against some known integrals. Functions to be integrated were evaluated at 20 or 40 variably spaced grid points, and cubic spline interpolation was used for intermediate points as required by the Gaussian or Romberg methods. More grid points were concentrated in regions where temperatures had the largest variations as determined by preliminary calculations. Time increments of $\Delta\tau = 0.005$ were used at the beginning of the calculations when quantities were changing rapidly with time. For some heating conditions the $\Delta\tau$ was increased to 0.01 and then to 0.02 later in the transient calculations. For large imposed heating it was sometimes necessary to retain a small $\Delta\tau$ such as 0.005 or 0.01 to maintain stability during the integration forward in time. To check the accuracy of forward extrapolation with time, a few calculations were duplicated using one-half the time increment. The time increments were small enough that the special forms in Eqs. (13) were valid. As will be shown, very good agreement was obtained with a previous transient numerical solution and with independently calculated solutions for steady state.

Results and Discussion

The purpose of this analysis was to develop and demonstrate a method using Green's functions for obtaining transient temperature distributions in parallel translucent layers including isotropic scattering, and for obtaining radiative exchange between layers. Using these functions provides analytical relations that include exact forms of the boundary conditions, as an alternative to finite difference or other numerical solution methods. The radiative energy source term in the transient energy equation was obtained by solving the two-flux equation by using a Green's function that incorporated the boundary conditions of externally incident radiation. Using the internal radiative heat source within each layer, the transient energy equation was solved with a Green's function that included the convective boundary conditions. The method is applied for parallel translucent layers by including the radiative exchange in the space between them as required for the boundary conditions for the radiative source.

The results shown first are for verification of the present transient solution method. Transient temperature distributions in a single layer are compared with previous transient calculations using the exact equations of radiative transfer and a finite difference method. Then another demonstration of the method is given to show the interesting transient situation of a layer that is being heated by convection while being simultaneously cooled by radiation to cold surroundings. Transient heating of two parallel layers is then illustrated, when they are separated by a space so that energy is transferred between them only by radiation from within the translucent materials. This is compared with transient heating when the two layers are combined into a single layer with the same heating and cooling conditions at the external boundaries. The transient temperature distributions given here begin with a uniform initial temperature $t(X, 0) = 1$, although the solution method can be applied for any $t(X, 0)$.

Results for a Single Layer

Typical results for transient temperature distributions in a single layer using the two-flux method and two Green's functions are in Fig. 2, as compared with $T(x, \Theta)/T_i$ from a semi-implicit finite difference method using the exact transfer equations to evaluate the radiative heat source in the transient energy equation.[4] The layer is heated at its hot side ($x = 0$) by the sudden application of a radiative flux from blackbody surroundings at $T_{s1} = 1.5T_i$, where T_i is the layer initial temperature, and there is no convection at $x = 0$. At the other side ($ax = a2D = 2$) the surroundings are at a lower temperature $T_{s2} = 0.5T_i$, so that there is cooling by radiation through that boundary combined with convective heat loss. These are possible conditions for a ceramic component in a combustion chamber where there is primarily radiative heating from combustion gases and soot on one side, and that side is not being film cooled. The layer optical thickness is 2, its refractive index is 2 (in the typical range for ceramics), and there is no scattering. The solid lines in Fig. 2 are transient temperature distributions from the present analysis, and the dashed lines are from Ref. 4, where the exact transfer equations and a finite difference method were used. The transient results illustrate the temperature response to radiant heating at $x = 0$, combined with convective and radiative cooling at $ax = 2$, that produce a signif-

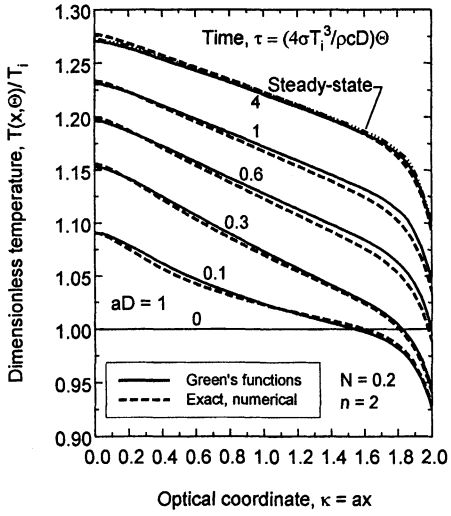

Fig. 2 Two-flux with Green's functions, and exact numerical results for transient temperatures in a gray layer initially at uniform temperature after exposure to radiation on one side and convective and radiative cooling on the other. Parameters: $aD = 1$ (D = layer half-thickness), $\Omega = 0$, $N = 0.2$, $n = 2$ ($\rho^i = 0.79015$, $\rho^o = 0.16060$), $\tilde{q}_{r1} = 1.5^4$, $\tilde{q}_{r2} = 0.5^4$, $H_1 = 0$, $H_2 = 1$, $t_{g2} = 0.5$.

icant temperature decrease near that boundary. The results from the present method agree very well with those from the exact equations.[4] The dot–dashed line shows the steady-state solution obtained by using the two-flux approximation in an analysis similar to that in Ref. 8. When $\tau = 4$, the transient temperature distributions are very close to steady state, and the transient solution is properly converging to the steady-state results. These results help verify the validity of the present method.

Before showing transient temperatures for two parallel layers, the results in Fig. 3 are another example illustrating the present method for a single layer and showing an interesting transient effect of radiation combined with convection. Before the transient begins, the layer has been heated to $T(x, 0) = T_i$ by equal convection on both sides with gas at temperatures $T_{g1} = T_{g2} = T_i$. The uniform initial temperature is at the upper boundary of Fig. 3. The layer is then suddenly exposed to surroundings where the radiative environment has a low effective blackbody temperature of $T_{s1} = T_{s2} = 0.2T_i$ on each side of the layer, so that the layer cools by radiative loss through both boundaries while still being heated by convection. As shown by the transient temperature distributions, the temperatures begin to decrease rather uniformly by radiative loss from a layer that is of moderate optical thickness so that radiation can leave from its interior. Conditions are the same on both sides of the layer, and so the transient temperatures are symmetric. During cooling, the gas temperature on each side remains at T_i, the initial elevated temperature of the layer. As temperatures decrease by radiative cooling from the layer interior, convection increases from the surrounding gas to the layer as a result of the increased difference between the gas and layer surface temperatures. As time increases, the combination of convective heating at the surfaces, and radiative cooling from the interior, produces interior temperatures that are lower than the surface values. The dashed horizontal line shows the uniform temperature that would be reached if the layer were opaque and had radiant emission and absorption only at its surfaces that have reflection properties for a dielectric with $n = 2$. At steady state, the translucent layer has lower internal temperatures than for an opaque layer, with the lowest temperatures in the central portion of the layer. The transient temperatures for large times are in good agreement with the steady-state temperature distribution independently predicted by using the method in Ref. 11 that applies for steady state with symmetric boundary conditions.

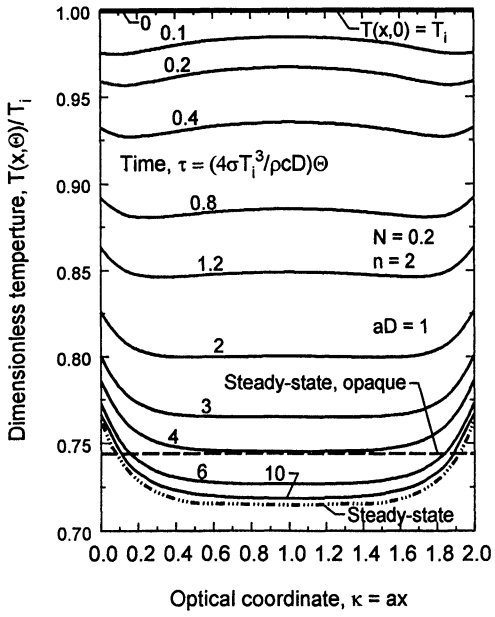

Fig. 3 Transient temperatures using Green's functions and two-flux method for internal radiative cooling of a layer in cold radiative surroundings with layer boundaries heated by convection. Parameters: $aD = 2$, $\Omega = 0$, $N = 0.2$, $n = 2$ ($\rho^i = 0.79015$, $\rho^o = 0.16060$), $\tilde{q}_{r1} = \tilde{q}_{r2} = 0.2^4$, $H_1 = H_2 = 1$, $t_{g1} = t_{g2} = 1$.

Results for Two Parallel Layers

The purpose of Fig. 4 is to investigate the insulating characteristics of a vacuum space between two translucent layers, and to show how this space influences transient heating by incident external radiation from one side. Compared with Fig. 2, the radiative flux incident at $x = 0$ for a single layer, or $x_1 = 0$ for two layers, is increased by a factor of approximately 3, with the other conditions and parameters remaining the same. The dashed lines show transient temperatures for a single layer with an optical thickness of 2, and results are compared at the same times with the solid lines that are for two equal parallel layers that each have an optical thickness of $a_jD = 1$. The two parallel layers are separated by a vacuum space with radiation exchanged across it from within the translucent layers as in Fig. 1. The dimensionless time is based on the thickness of one parallel layer that equals the half-thickness of the single layer corresponding to the dashed lines. The steady-state distributions for two layers, and for a single layer, were computed independently using the methods in Refs. 9 and 8, and are shown by the dot–dashed lines. When the dimensionless time reaches $\tau = 1$, the transient temperatures are close to the steady-state values. The steady-state temperatures for a single layer fall between those for two parallel layers. Consider the solid lines for the two-layer transient: at $\tau = 0.1$, the temperatures in the first layer have increased rapidly and are above the values for a single layer. For the second layer, however, convective and radiative cooling have produced decreased temperatures near $a_1D + a_2D = 2$. At $\tau = 0.1$, there is very little radiation across the space between the layers as a result of the temperatures still being low. At $\tau = 0.2$, the temperatures in the first layer are high enough that the second layer has started to increase in temperature. Throughout the transient the second layer has a much slower response with

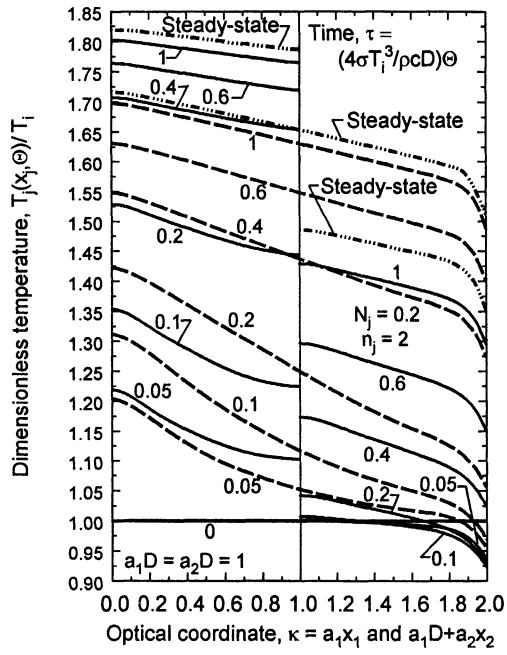

Fig. 4 Transient temperatures in two parallel translucent layers separated by a vacuum space, as compared with a single layer with the same combined thickness; layers initially at uniform temperature are exposed to radiative heating on one side and convective and radiative cooling at the other. Parameters: for one layer, $aD = 1$ (D = layer half-thickness), $N = 0.2$, $n = 2$, $\tilde{q}_{r1} = 2^4$, $\tilde{q}_{r2} = 0.5^4$, $H_1 = 0$, $H_2 = 1$, $t_{g1} = 1$, $t_{g2} = 0.5$; for two layers, $a_jD = 1$, $N_j = 0.2$, $n_j = 2$, $\tilde{q}_{r11} = 2^4$, $\tilde{q}_{r22} = 0.5^4$, $H_{11} = H_{12} = H_{21} = 0$, $H_{22} = 1$, $t_{g22} = 0.5$.

temperatures considerably below those in the first layer or in the single layer. The space between layers provides considerable reduction in transient heating of the second layer. Throughout the transient heating there is a large temperature decrease from the first to the second layer.

To show the effect of stronger heating at $x = 0$ for a single layer, or at $x_1 = 0$ for two layers, and also to illustrate the effect of scattering, the incident radiative flux at $x = x_1 = 0$ for Figs. 5 and 6 has been increased by a factor of about 5 from that in Fig. 4, and convective heating at $x = x_1 = 0$ has been added. Figure 5 is without scattering, and the single and dual layers are shown in Figs. 5a and 5b using the same size temperature scale for comparisons. With higher radiation, and convective heating added, the temperatures increase more rapidly than in Fig. 4, and there is a temperature gradient at $x = x_1 = 0$ compared with Fig. 4, where the boundary condition in Eq. (3a) provided a zero-temperature derivative. The increase in temperature level provided by stronger heating provides greater radiative transfer across the space between the two layers, and temperatures in the second layer increase more rapidly. There is still a large temperature decrease from the first to the second layer.

To more fully examine the transient heating process, the internal radiative heat source distribution in the energy equation [the second term on the right of Eq. (1)] is shown in Fig. 5c as a function of time for the two-layer transient in Fig. 5b. At $\tau = 0$, just after heating is applied, there is a large heat source by radiation absorption near $x_1 = 0$, the source decreases

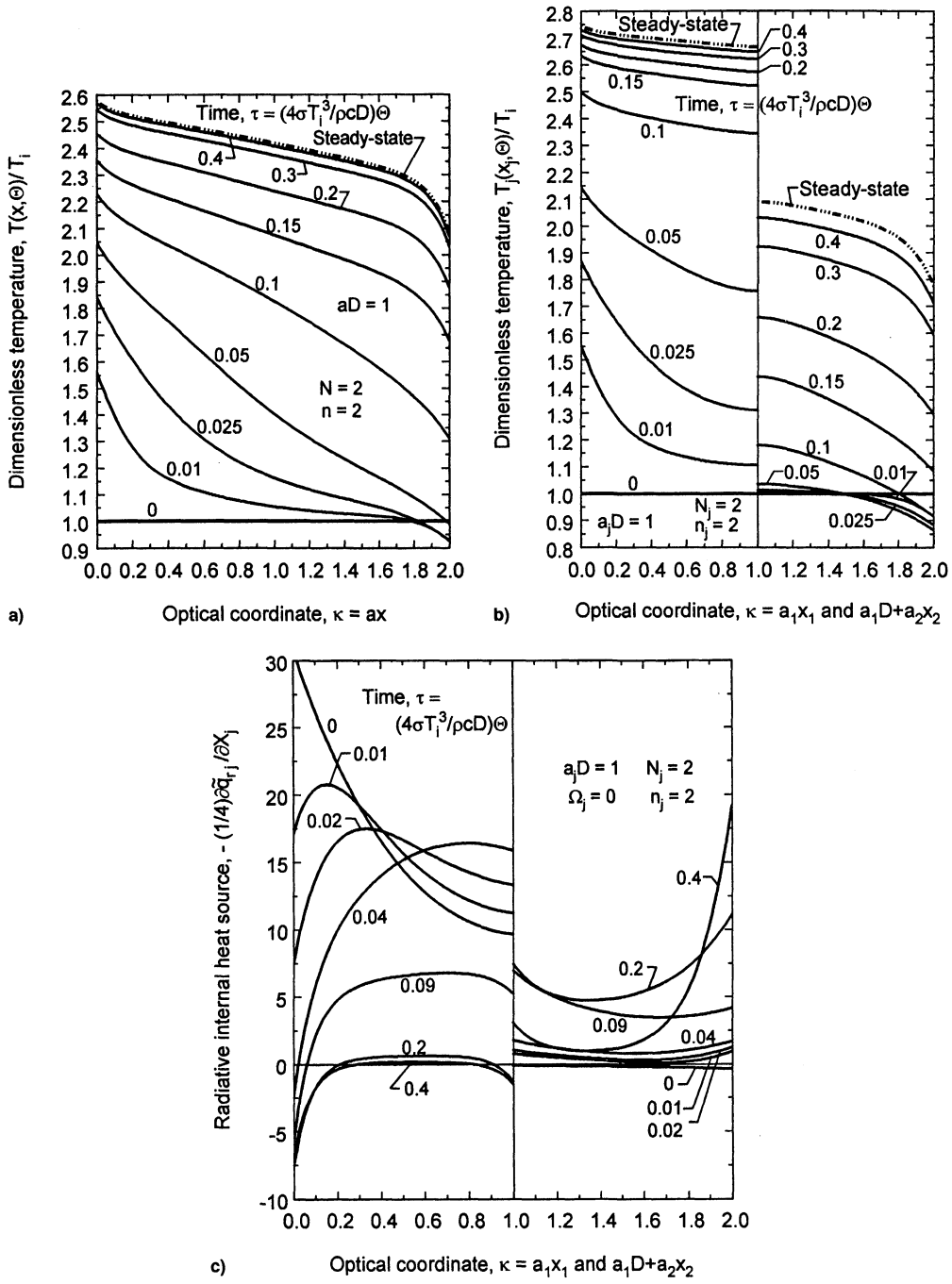

Fig. 5 Comparison of transient temperatures in two parallel translucent layers separated by a vacuum space, with a single layer having the same combined thickness; layers initially at uniform temperature are exposed to radiative and convective heating on one side and convective and radiative cooling at the other: a) single layer with parameters: $aD = 1$ (D = layer half-thickness), $N = 2$, $n = 2$, $\tilde{q}_{r1} = 3^4$, $\tilde{q}_{r2} = 0.5^4$, $H_1 = H_2 = 10$, $t_{g1} = 1$, $t_{g2} = 0.5$; b) two layers with $a_jD = 1$, $\Omega_j = 0$, $N_j = 2$, $n_j = 2$, $\tilde{q}_{r11} = 3^4$, $\tilde{q}_{r22} = 0.5^4$, $H_{11} = 10$, $H_{12} = H_{21} = 0$, $H_{22} = 10$, $t_{g11} = 3$, $t_{g22} = 0.5$; and c) radiative internal energy source distributions for heating two layers.

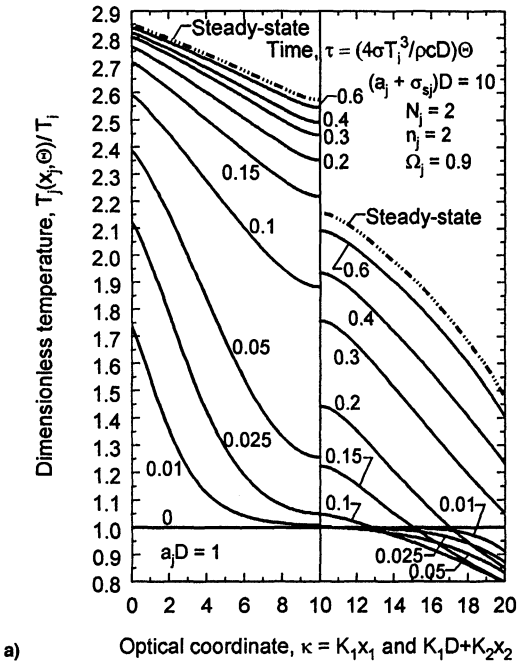

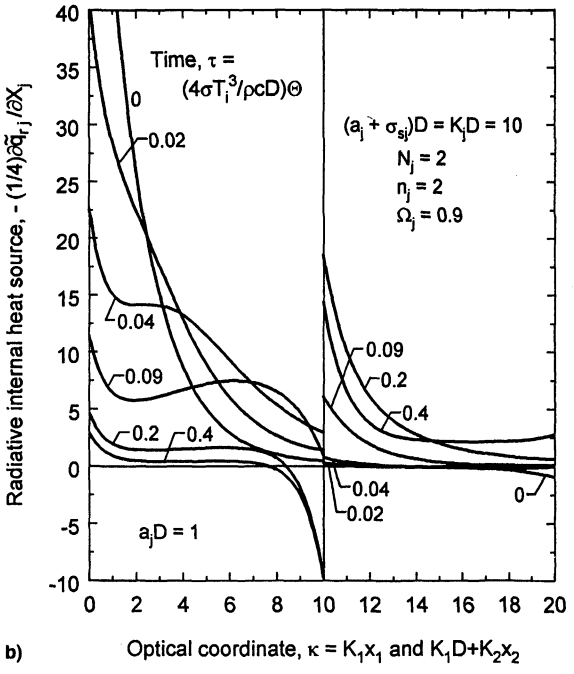

Fig. 6 Effect of isotropic scattering on transient temperatures in two parallel translucent layers separated by a vacuum space; layers start at uniform temperature and are subjected to radiative and convective heating on one side and to convective and radiative cooling at the other: a) transient temperatures and b) radiative internal heat source distributions. Parameters: $(a_j + \sigma_{sj})D = 10$, $\Omega_j = 0.9$, $N_j = 2$, $n_j = 2$, $\tilde{q}_{r11} = 3^4$, $\tilde{q}_{r22} = 0.5^4$, $H_{11} = 10$, $H_{12} = H_{21} = 0$, $H_{22} = 10$, $t_{g11} = 3$, $t_{g22} = 0.5$.

with increasing distance from the surface, and very little energy is received in the second layer. The heat source in the second layer is very slightly negative as a result of radiative cooling through the boundary at $a_1D + a_2D = 2$ that is exposed to a lower temperature $T_{s2} = 0.5T_i$. As heating by convection at $x_1 = 0$ raises the surface temperature as shown in Fig. 5b, the elevated internal temperatures near $x_1 = 0$ begin to provide a radiative loss so that the radiative source near $x_1 = 0$ decreases with time. For increased time as steady state is approached, the radiative source approaches zero in the central portion of the first layer, indicating that reradiation is balancing radiation absorbed from the external source. Temperatures in the first layer become almost linear as dominated by conduction. As temperatures increase in the first layer, radiation increases across the separation space, and the radiative source in the second layer increases. Reflections of internal radiation at a boundary can increase absorption in the region near the boundary for some conditions; this influences the shape of the radiative source distribution for $\tau = 0.4$ in the second layer in Fig. 5c. Near steady state, the radiative source becomes small in a portion of the second layer, indicating that internal emission is balancing absorption.

The effect of adding scattering in both layers is illustrated in Fig. 6, where the heating conditions are the same as those for Fig. 5. Scattering has been added with absorption kept the same. For an albedo of 0.9, this increases the optical thickness in each layer to $(a_j + \sigma_{sj})D = 10$, where $a_jD = 1$, as in Fig. 5b. Comparing Fig. 6a with Fig. 5b, the increased optical thickness as a result of added scattering produces steeper temperature gradients near $x_1 = 0$, as a result of decreased penetration of externally incident radiation. The internal radiative heat source is increased near $x_1 = 0$ as shown in Fig. 6b, and the transient source distributions are considerably different than in Fig. 5c as a result of stronger absorption near $x_1 = 0$. The transient temperature response of the second layer is reduced by decreased radiative penetration in the first layer. The temperature does not rise as rapidly at the boundary of the first layer adjacent to the separation space (at $K_1x_1 = 10$), so that radiation to the second layer is decreased. Radiation does not penetrate as well into the second layer, and so the source in Fig. 6b is highest near $x_2 = 0$. The parameters used here are in typical ranges where radiation effects are of the same order as convection and conduction. Because these results are for a scattering layer, an approximate physical interpretation can be made relative to zirconia that has scattering, keeping in mind that for more precise results, zirconia requires a two-band calculation.[8] Zirconia has a refractive index of approximately $n = 2$, as used here. Using $k = 0.8$ W/mK, as is characteristic of zirconia, $T_i = 700$ K, $a = 30$ m^{-1}, $\sigma_s = 2000$ m^{-1}, $h = 200$ W/m^2 K, and a thickness of $D = 0.005$ m gives $H = 10.3$, $N = 2.1$, $\kappa_D = 10.2$, and $\Omega = 0.985$, that are in the parameter range used for Fig. 6.

Conclusions

A method was developed using two Green's function solutions to obtain transient temperatures in two parallel translucent layers separated by a space across which there is only radiation exchange from within the translucent media. Each layer has internal radiative absorption, emission, and scattering, in addition to heat conduction. Starting from an initial temperature distribution that can have an arbitrary shape, the layers undergo transient heating or cooling by external radiation and convection. A Green's function is used to solve the two-flux equation for the internal radiation source in each layer during the transient, and another Green's function was used to solve the transient energy equation. Determining temperature distributions requires accurate evaluations of the integrals containing Green's functions. The method is an alternative to using a finite difference procedure, and can be used to help verify numerical solutions. Evaluating the integrals requires increased computer time relative to using finite differences, but the expressions are in analytical forms that incorporate the boundary conditions and do not require numerical approximations near the boundaries.

Transient temperature distributions from the present method were compared for a single layer, with results where the radiative heat source in the transient energy equation was evaluated numerically from the exact radiative transfer equations, and a semi-implicit finite difference solution was used for the energy equation. Good agreement of the present method was obtained with the numerical solution. An illustrative solution was given for transient temperatures in a single layer that is

convectively heated while simultaneously being subjected to cold surroundings that provide radiative cooling from within the translucent layer. This produces interior temperatures lower than the surface temperatures. The transient solution for two parallel translucent layers is compared with a single layer having the same total optical thickness, and with its boundaries subjected to the same thermal conditions as the external boundaries of the two-layer combination. The thermal resistance of an evacuated internal space between the two layers produces substantially different temperatures than for a single layer. If the first layer is being heated, the thermal response of the second layer is substantially reduced; there is no heat conduction across the internal space, and energy must be transferred by radiation between the two translucent materials.

References

[1]Field, R. E., and Viskanta, R., "Measurement and Prediction of Dynamic Temperatures in Unsymmetrically Cooled Glass Windows," *Journal of Thermophysics and Heat Transfer*, Vol. 7, No. 4, 1993, pp. 616–623.

[2]Lee, K. H., and Viskanta, R., "Transient Conductive–Radiative Cooling of an Optical Quality Glass Disk," *International Journal of Heat and Mass Transfer*, Vol. 41, No. 14, 1998, pp. 2083–2096.

[3]Siegel, R., "Transient Thermal Effects of Radiant Energy in Translucent Materials," *Journal of Heat Transfer*, Vol. 120, No. 1, 1998, pp. 4–23.

[4]Siegel, R., "Transient Heat Transfer in a Semitransparent Radiating Layer with Boundary Convection and Surface Reflections," *International Journal of Heat and Mass Transfer*, Vol. 39, No. 1, 1996, pp. 69–79.

[5]Chang, Y. P., and Smith, R. S., Jr., "Steady and Transient Heat Transfer by Radiation and Conduction in a Medium Bounded by Two Coaxial Cylindrical Surfaces," *International Journal of Heat and Mass Transfer*, Vol. 13, No. 1, 1970, pp. 69–80.

[6]Siegel, R., "Two-Flux and Green's Function Method for Transient Radiative Transfer in a Semitransparent Layer," *Radiative Transfer—I*, Begell House, New York, 1996, pp. 473–487.

[7]Siegel, R., and Spuckler, C. M., "Approximate Solution Methods for Spectral Radiative Transfer in High Refractive Index Layers," *International Journal of Heat and Mass Transfer*, Vol. 37 (Suppl. 1), 1994, pp. 403–413.

[8]Siegel, R., "Internal Radiation Effects in Zirconia Thermal Barrier Coatings," *Journal of Thermophysics and Heat Transfer*," Vol. 10, No. 4, 1996, pp. 707–709.

[9]Siegel, R., "Radiative Exchange in a Parallel-Plate Enclosure with Translucent Protective Coatings on Its Walls," *International Journal of Heat and Mass Transfer* (to be published).

[10]Beck, J. V., Cole, K. D., Haji-Sheikh, A., and Litkouhi, B., *Heat Conduction Using Green's Functions*, Hemisphere, Washington, DC, 1992, pp. 18, 43, and 503.

[11]Siegel, R., and Spuckler, C. M., "Temperature Distributions in Semitransparent Coatings—A Special Two-Flux Solution," *Journal of Thermophysics and Heat Transfer*," Vol. 10, No. 4, 1996, pp. 39–46.